Evolution of plasma turbulence in the solar wind and near Earth' space

E. Yordanova

Swedish Institute of Space Physics, Uppsala, SWEDEN

In collaboration with:

M. André
A. Balogh
V. Carbone
G. Consolini
S. Perri
B. Popielawska
L. Sorriso-Valvo
A. Vaivads
A. Wernik

- ❑ Motivation
- ❑ Region of interest
- ❑ Spacecraft observations of turbulence in:
  - solar wind
  - magnetosheath
  - foreshock
  - high-altitude cusp

A 3D picture of the continuous turbulence development through multiscale regions from direct measurements

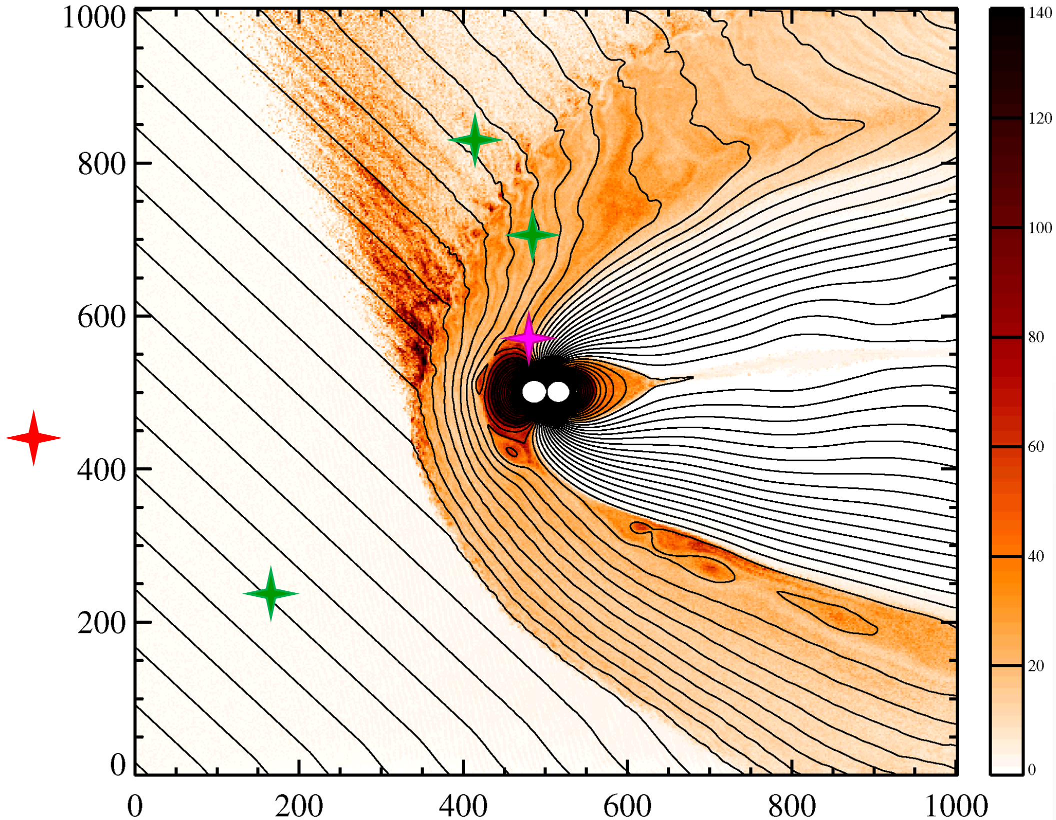

2-D Global Hybrid Simulations (D. Krauss-Varban, SSL, Berkeley)

- solar wind
- bow shock
- magnetosheath
- magnetopause
- cusp

Ulysses

Cluster

Polar

Near Earth' space

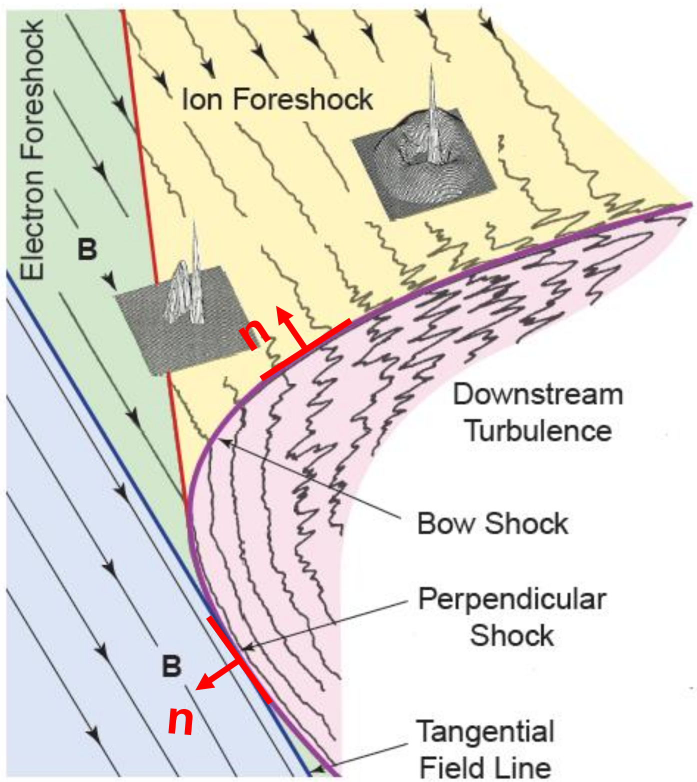

Eastwood et al., SSR, 2005

Solar wind – *supersonic* and *superalfvén* outflow of *e*- and *p*+

Foreshock – reflected by the bow shock electrons and ions; ULF waves; wave-particle interactions

Magnetosheath – heated and slowed down solar wind plasma; magnetic field and plasma fluctuations intensified downstream quasi-parallel shock

The Earth's magnetopshere

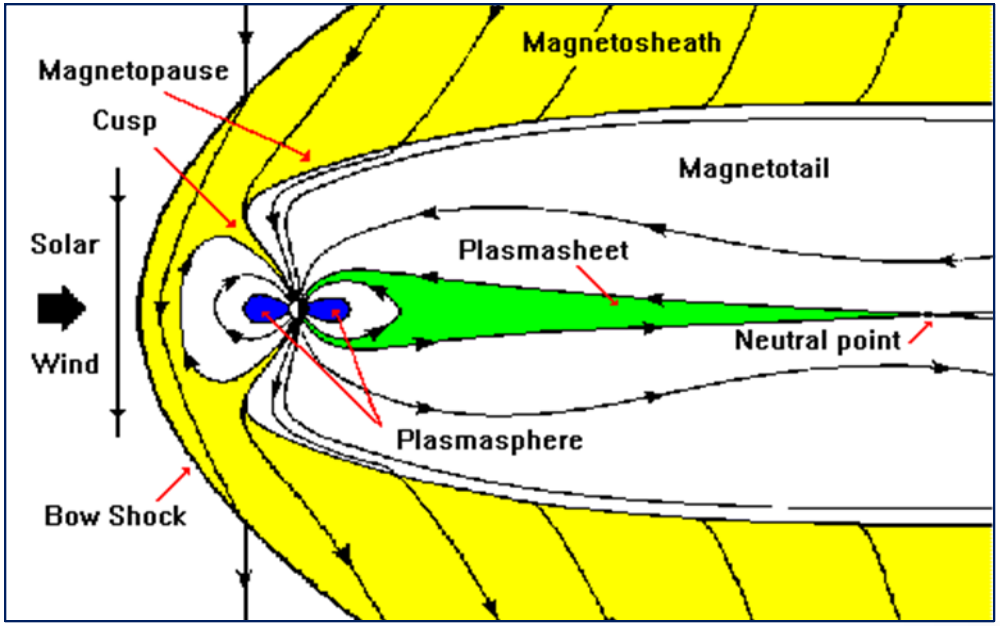

Picture NASA

The Earth's cusp

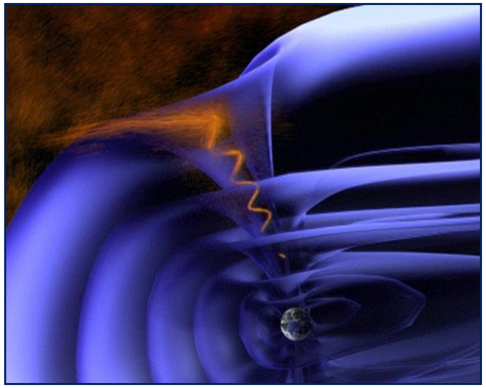

Picture ESA

Cusp – depressed and irregular magnetic magnetic field; magnetosheath plasma; plasma of ionospheric origin

Magnetopause – boundary separating solar wind and magnetospheric plasma

Near Earth space – complex, highly fluctuating, non-stationary, assumptions fail.

- Solar wind fluctuations and magnetic field are highly non-uniform

    - *depend on location and time and heliospheric conditions*
    - *dynamical interaction different solar wind fast and slow streams*
    - *differences in the fast or slow streams*
    - *differences within the same stream (fast or slow)*

- Solar wind type is best determined from the distribution of charge states of oxygen ions (O^{+7}/O^{+6} - coronal temperature) rather than from kinetic parameters

- Ulysses data (equatorial plane, polar regions from Sun to Jupiter) *'pure' slow* – long periods of low speed

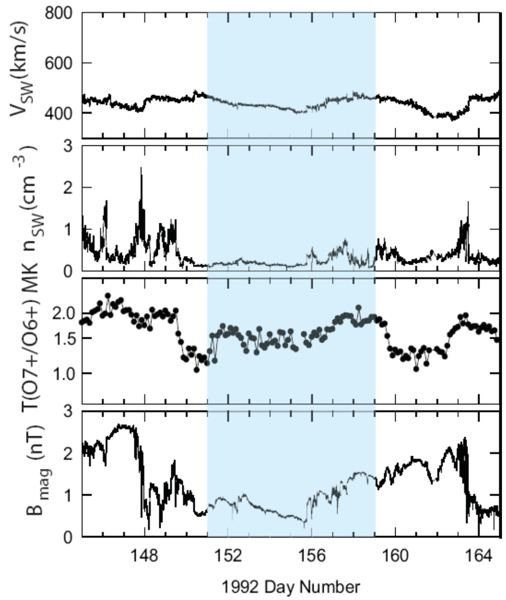

slow streams – low speed separated from the mixed

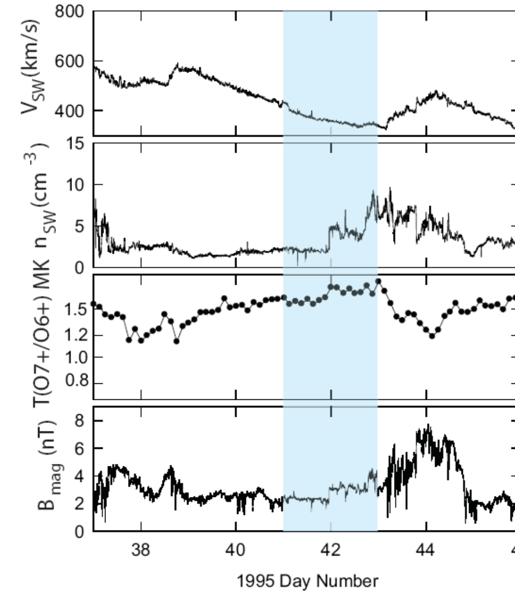

'pure' fast – polar fast wind

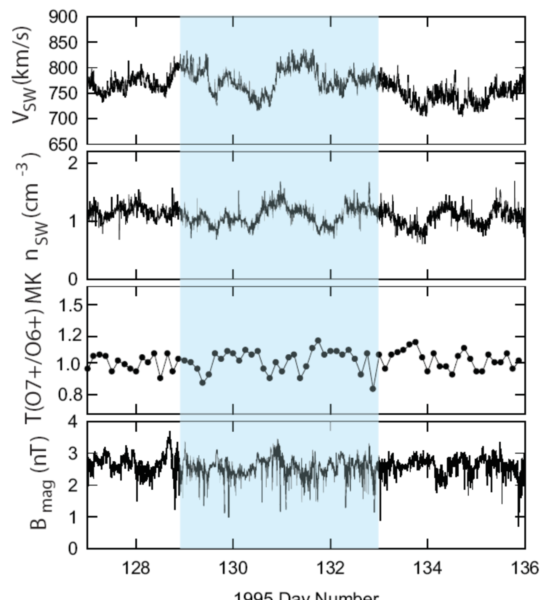

fast streams – high speed separated from the mixed

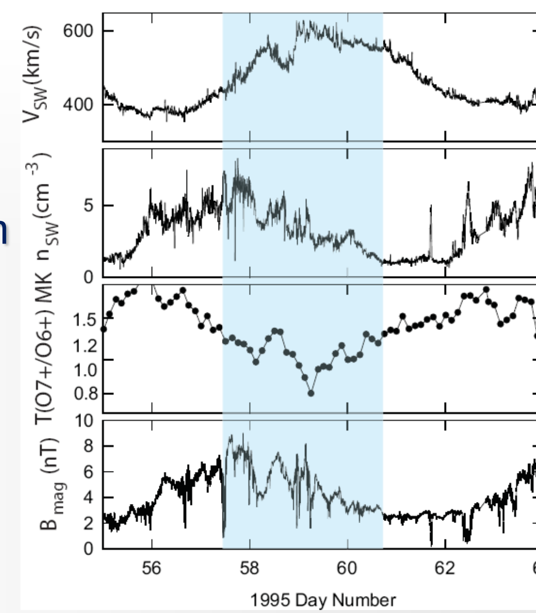

[Yordanova et al., 2009, JGR]

- Power spectra $P(f)$

- Structure functions $S^n(\vec{r}) = \left\langle \left| \vec{b}_i(\vec{x}+\vec{r}) - \vec{b}_i(\vec{x}) \right|^n \right\rangle$

(differences of the field separated by a distance r represents characteristic fluctuations at the scale r)

- Flatness $F(\vec{r}) = \dfrac{\left\langle S^4(\vec{r}) \right\rangle}{\left\langle S^2(\vec{r}) \right\rangle^2}$

(the signal is intermittent if the flatness increases toward the smaller and smaller scales)

Taylor hypothesis $f = 1/\Delta t$ $k = 2\pi f / V_{SW}$

Magnetic field Ulysses, 1995

Decreasing the window (*scale*) the intense fluctuations become more visible and important

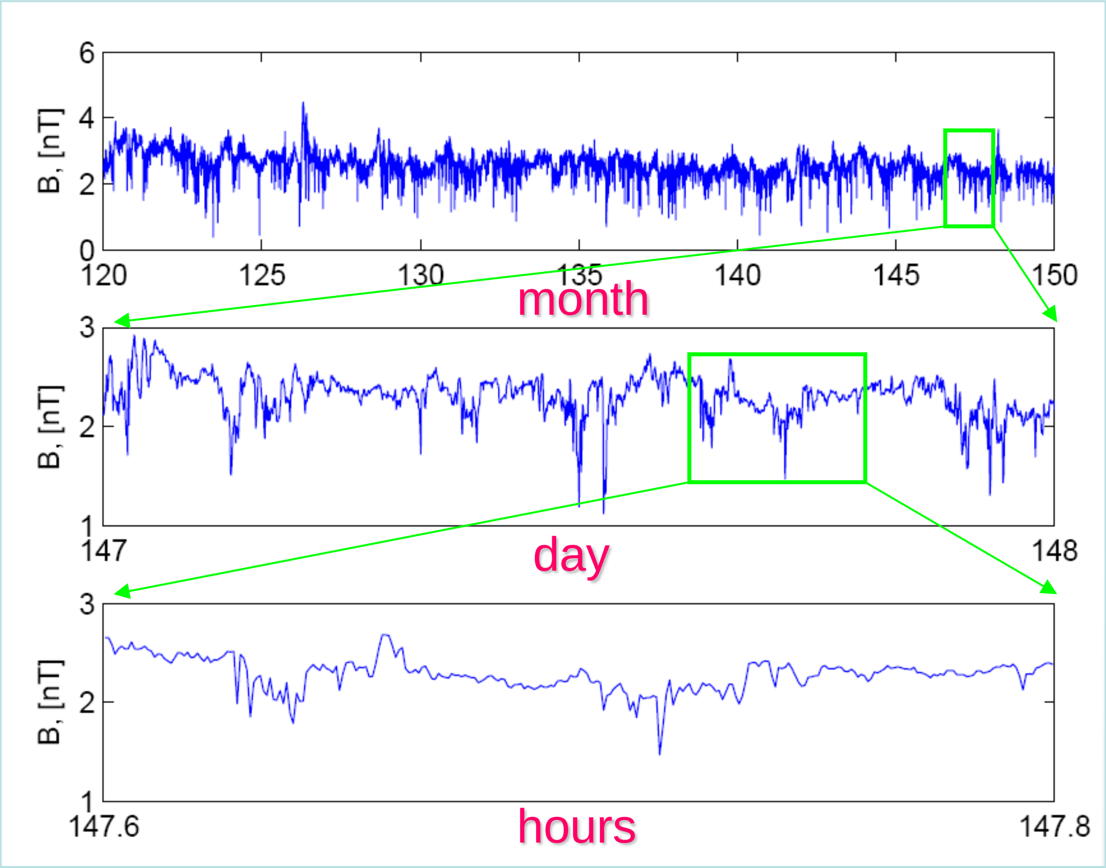

ULYSSES OBSERVATIONS

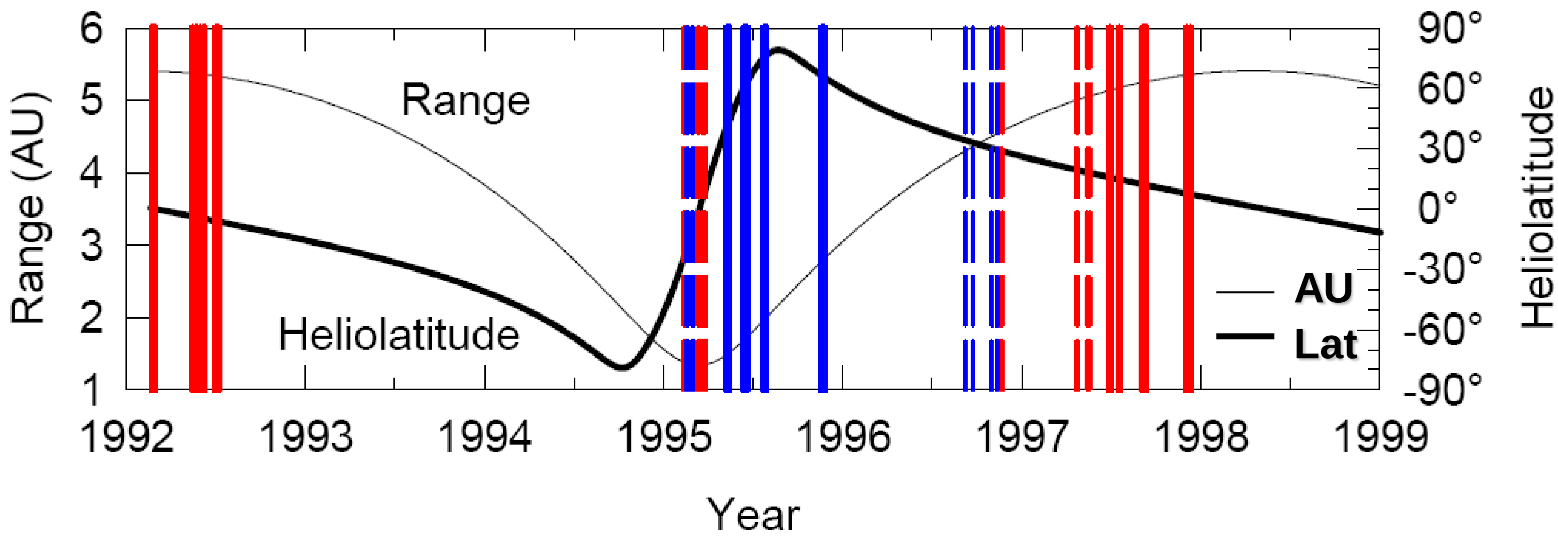

21 data samples

25°S - 80°N

1.5 – 5.4 AU

Pure slow
Slow stream
Pure fast
Fast stream

“Pure” slow wind

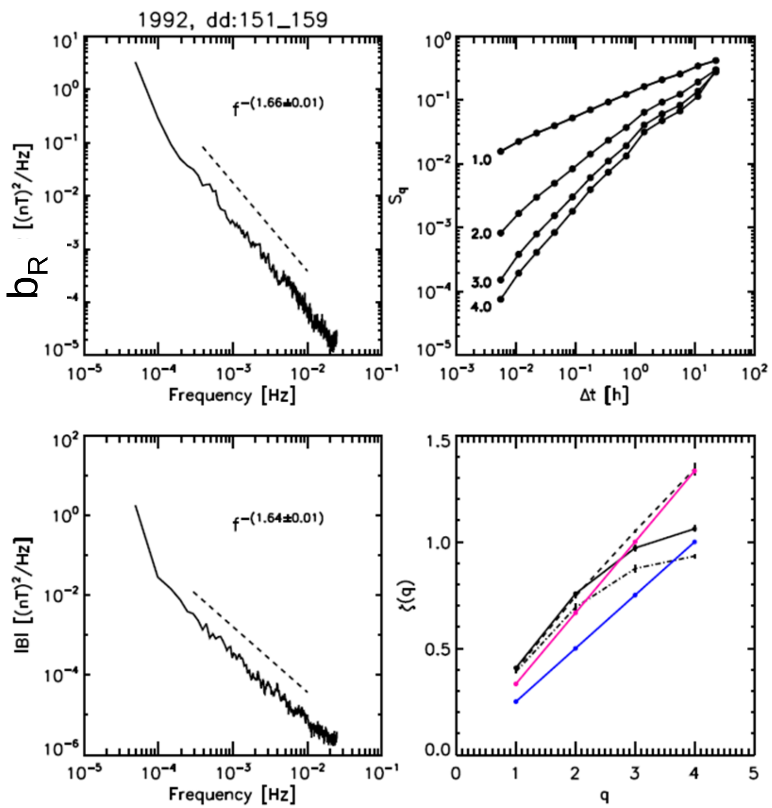

Fast stream

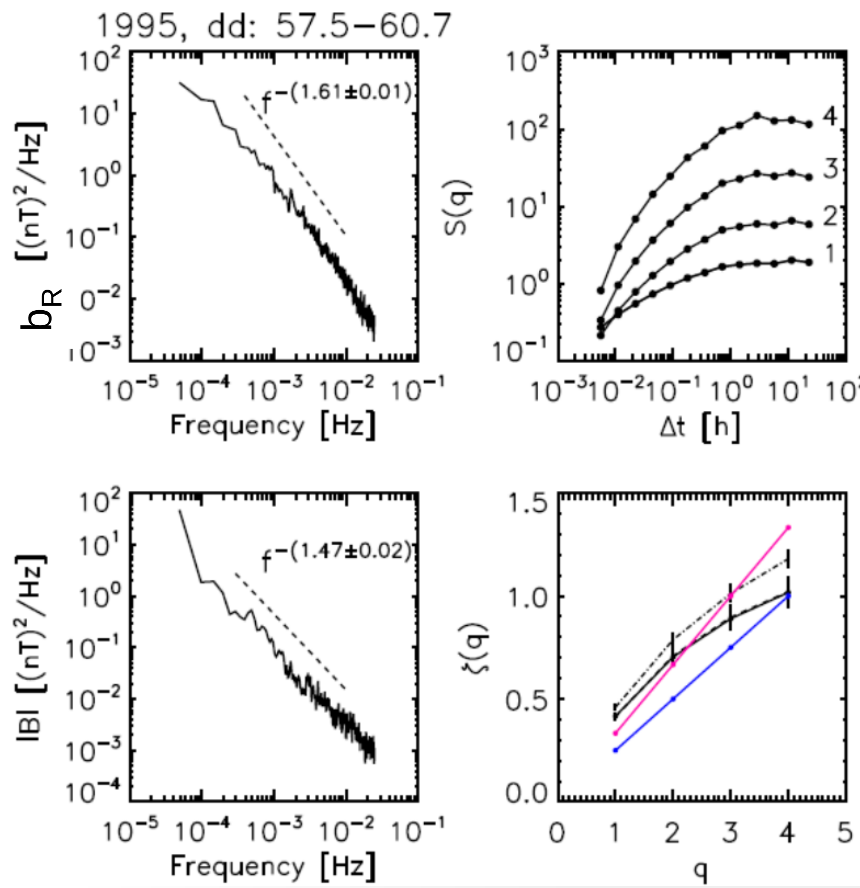

b_R ———
b_T – – –
b_N – · – ·

KO
KI

SOLAR WIND. FLATNESS

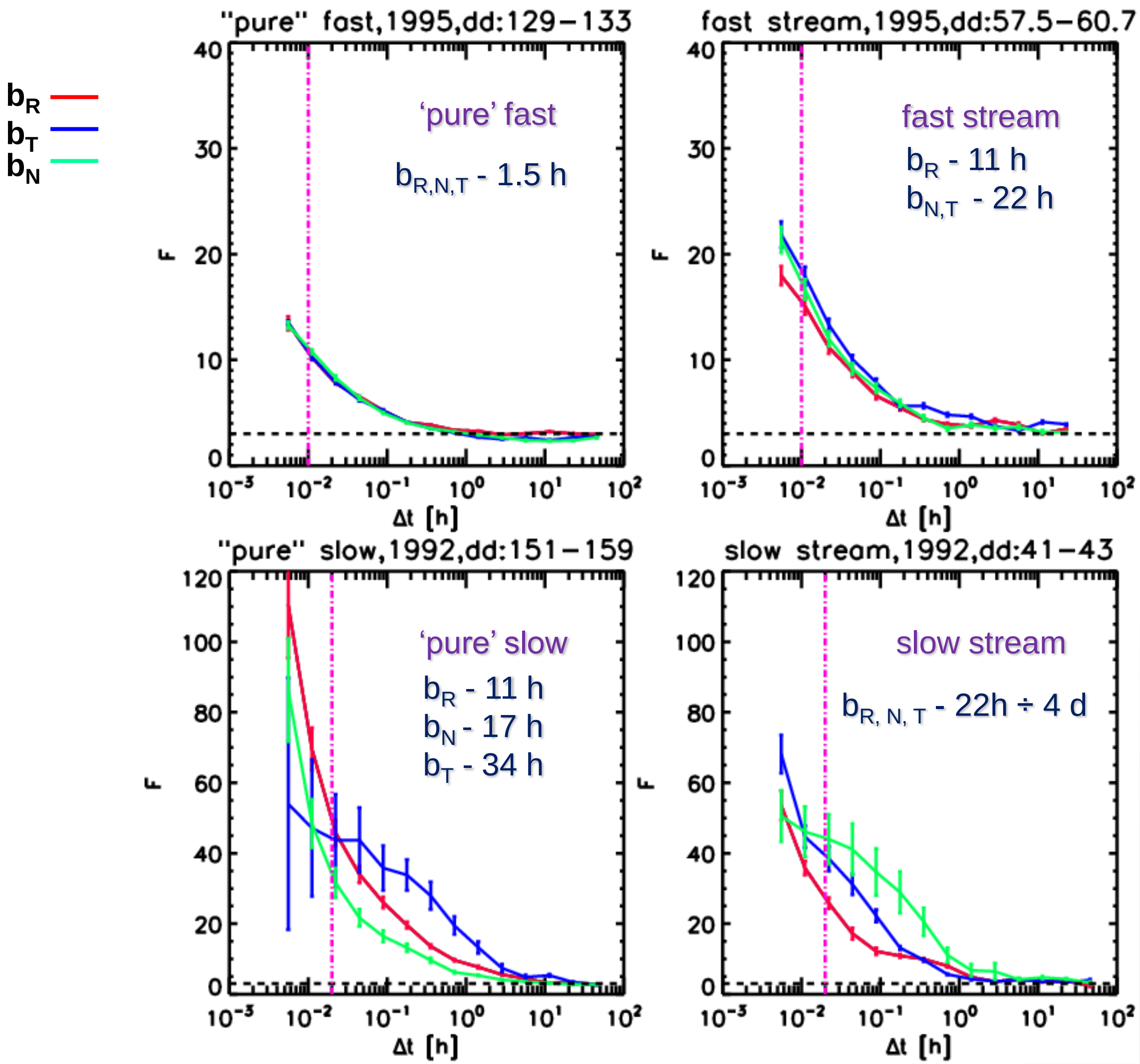

Δt = 0.01 h *fast* (780 km/s)

Δt = 0.02 h *slow* (430 km/s)

F = 3 (Gaussian)

	PSD b_R b_T b_N |B|	Flatness b_R b_T b_N	Lat AU
Pure fast	1.63 1.65 1.66 1.31 (*1/f*-like)	8.2 8.3 8.9	10°S – 10°N, 5.4
Fast streams	1.64 1.68 1.71 1.48 (*Kraichnan*-like)	16.1 16.2 15.2	25°S – 30°N, 1.5 - 5
Pure slow	1.66 1.68 1.66 1.68 (*Kolmogorov*-like)	25.5 35.5 23.1	50°S – 80°N, 1.5 - 3
Slow streams	1.76 1.82 1.69 1.73 (~ *1.8*)	17.3 25.2 19.2	10°S – 30°N, 1.5 - 4.5

Δt = 0.01 h fast (780 km/s)

Δt= 0.02 slow (430 km/s)

Conclusions

- Turbulence nature – for different solar wind types is different, because of the different region of origin in the solar corona.
  - fast wind – slowly developing turbulence
  - slow wind - developed turbulence
- Intermittency – regardless of the type of the solar wind, the turbulence is intermittent.
  - *least* intermittent is the pure fast wind
  - *most* intermittent is the pure slow wind
  - fast streams *less* intermittent than slow streams
- Radial evolution – pure fast wind evolves towards MHD-like turbulence and it is the only type showing evolution; higher estimation of flatness.
- Solar activity – during and close to solar minimum we can observe different solar wind types; around solar maximum expect turbulence properties similar to the pure slow wind.

Turbulence behind a quasi-parallel shock

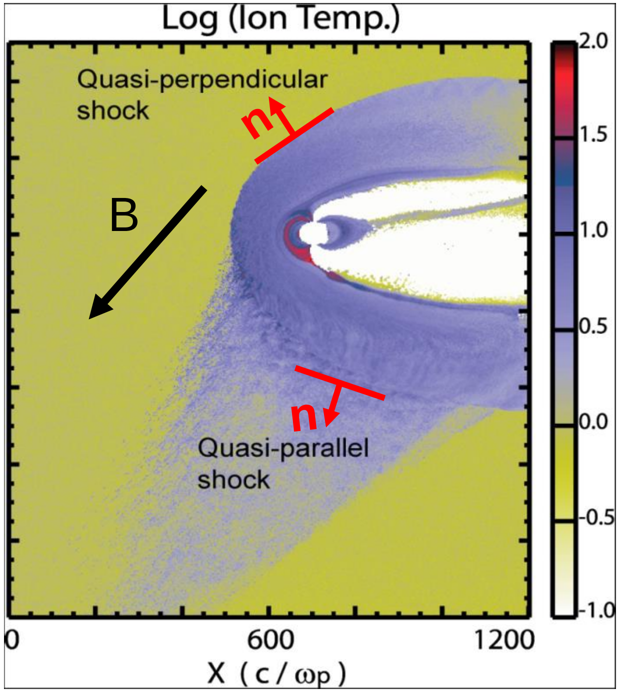

[Omidi et al., 2005, JGR]

2003, April 16

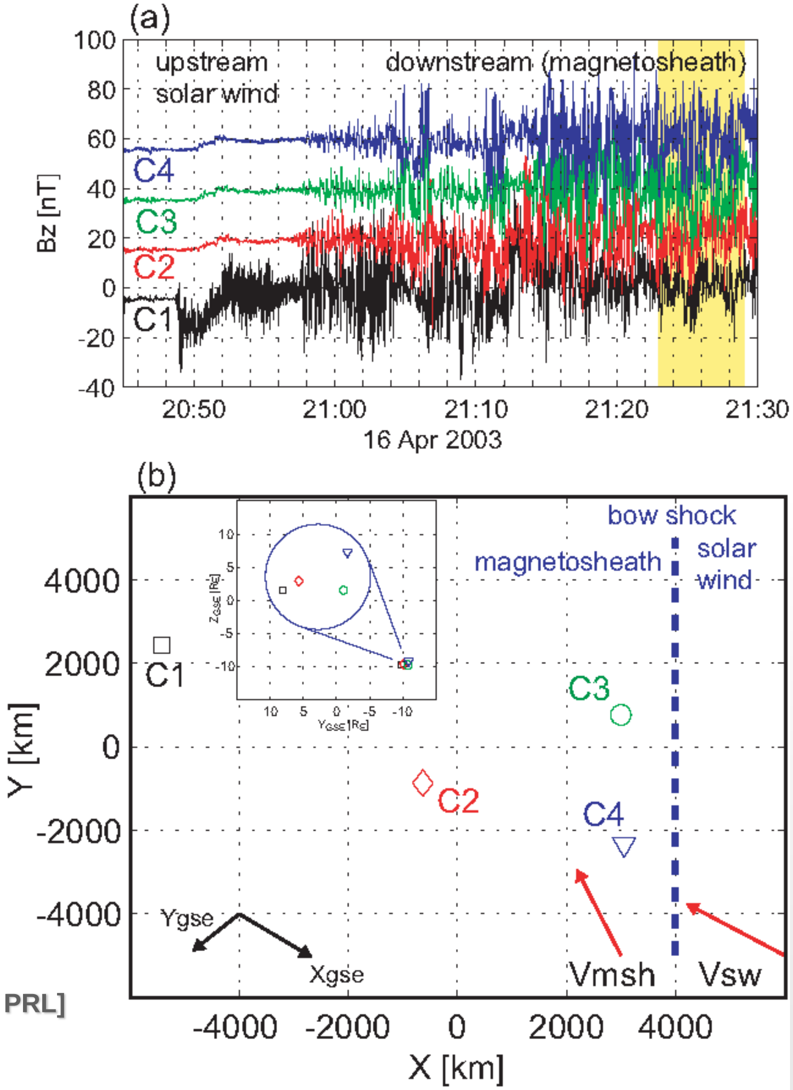

[Yordanova et al., 2008, PRL]

Power spectral density

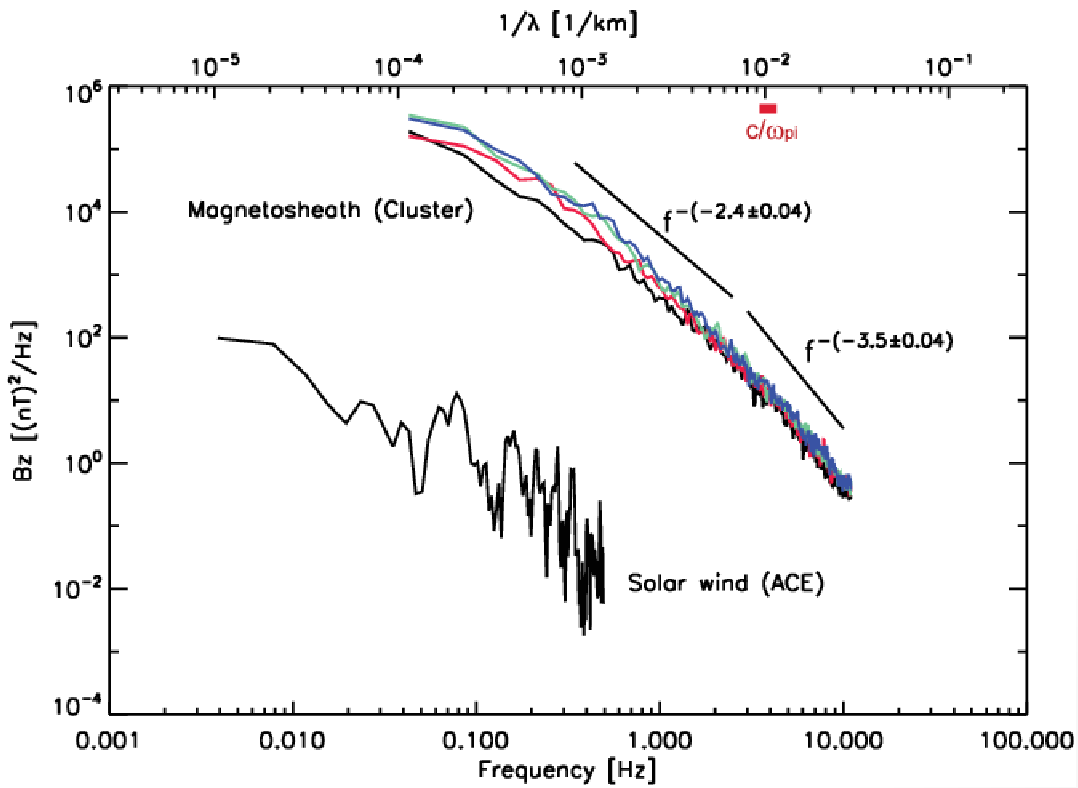

(0.33 – 2.5 Hz)

0.3 – 4 s

150 -1100 km

2 - 15 c/ω_{pi}

(V_{msh} ~ 375 km/s)

Wavelet based partition function (Muzy et al., 1991):

$$Z(q,a) \sim a^{\tau(q)}, \qquad Z(q,a) = \sum_{l \in L(a)} \left(\sup_{a' \le a} \left| T_\psi [g] (b_l(a'), a') \right| \right)^q$$

L*(*a*)** - a set of all the maxima lines ***l existing at a scale ***a***; ***b*$_l$(*a*)** - the position, at ***a***, of the maximum belonging to the line ***l***

Scaling exponents of PF

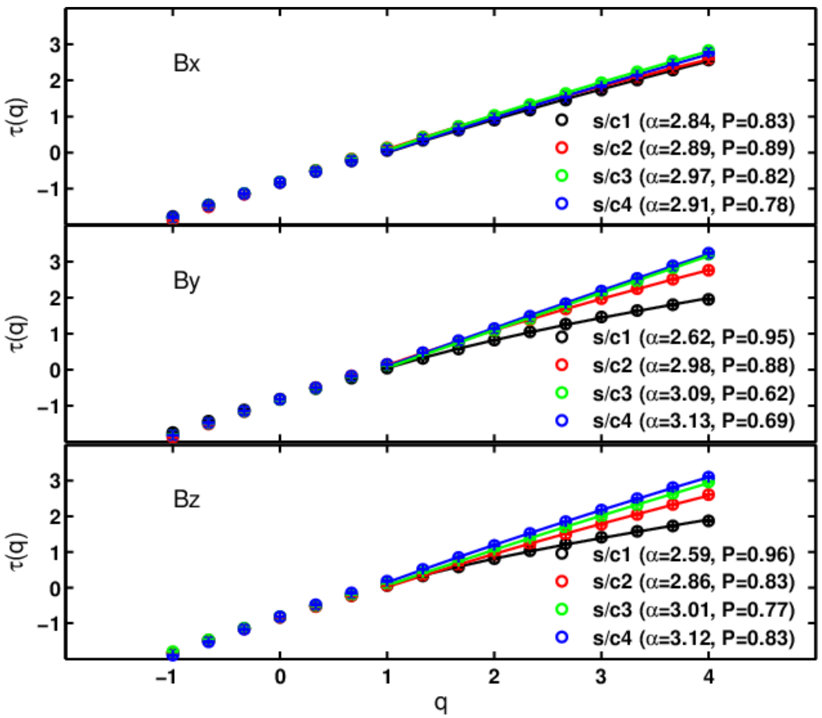

Models

1. P-model (Meneveau & Sreenivasan, '87,'91):

$$\tau(q) = -\log_2 \left[P^{\varsigma_q} - (1-P)^{\varsigma_q} \right]$$

$P_1 = 0.5$ - no intermittency
$P_1 = 1$ - fully intermittent case

2. Extended SF (Tu et al., '96, Marsh &Tu, '97):

$$\tau(q) = \left(-\frac{5}{2} + \frac{3}{2}\alpha \right) \frac{q}{3} - \log_2 \left[P^{q/3} + (1-P)^{q/3} \right]$$

(Kolmogorov-like cascade)

$$\tau(q) = (-3 + 2\alpha) \frac{q}{4} - \log_2 \left[P^{q/4} + (1-P)^{q/4} \right]$$

(Kraichnan-like cascade)

Conclusions

P and α vs distance from the bow shock

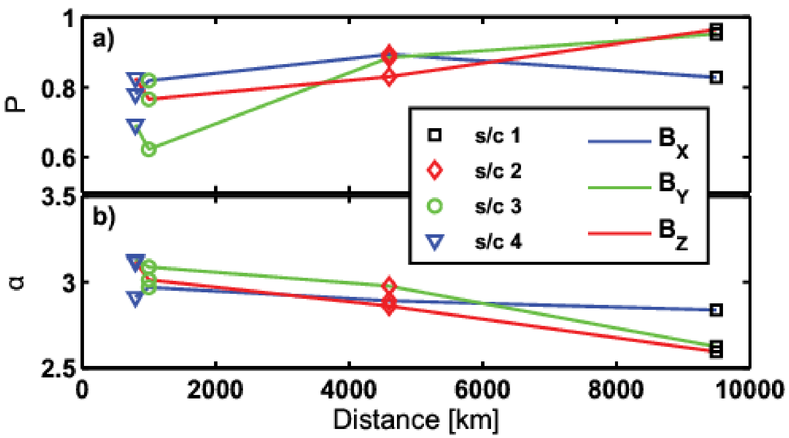

- The magnetosheath turbulence at spatial scales 2-15 c/ω_{pi} is *not in a fully developed state* after the shock crossing.
- There is a clear *anisotropy* of the turbulence with respect to the shock normal
- There is *small intermittency* and *no anisotropy* in the frequency range between 3-10 Hz (25-125 km)

Magnetic field turbulence in the solar wind, foreshock and magnetosheath

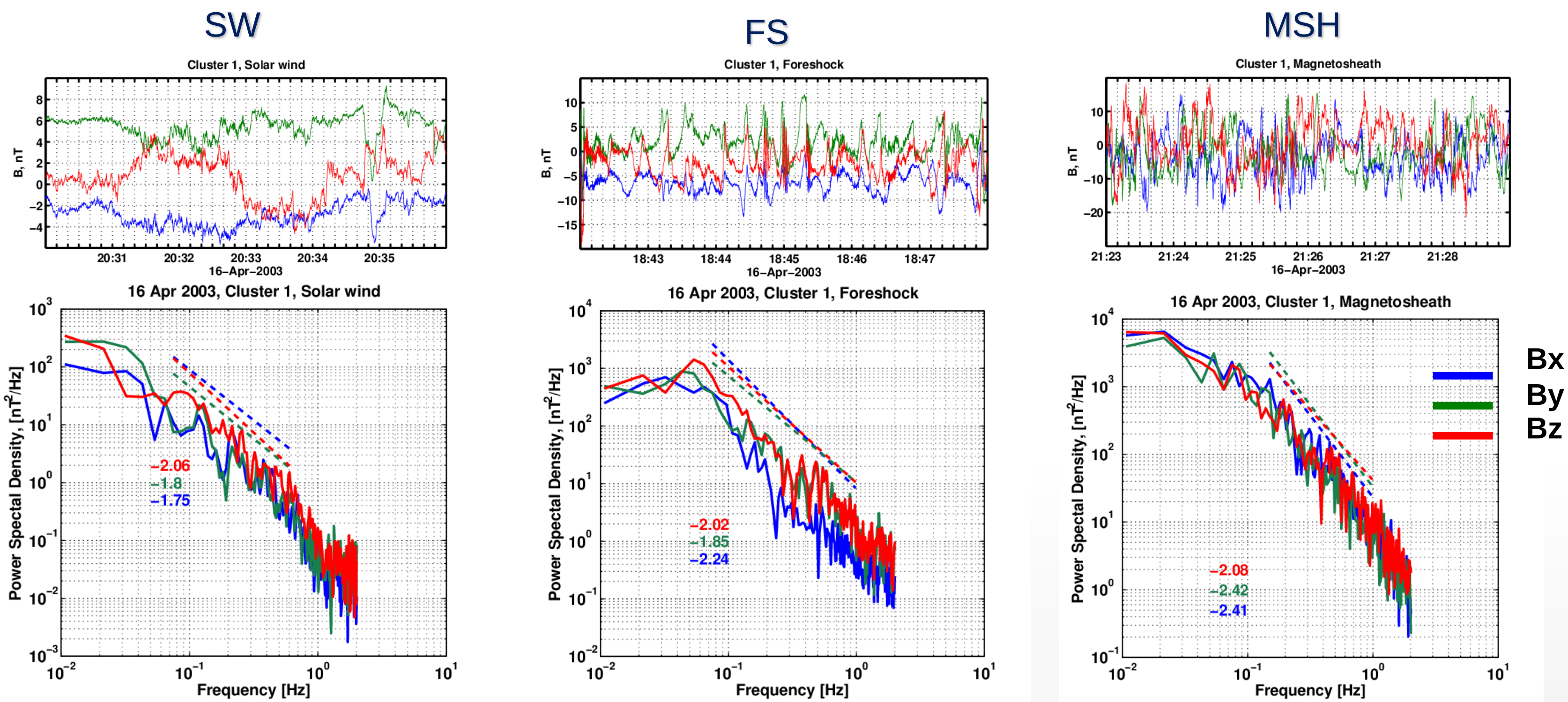

Region	$\langle v \rangle$ (Km/sec)	B_0 (nT)	$\langle n \rangle$ (cm^{-3})	$\langle T_i \rangle$ (eV)	$\langle T_e \rangle$ (eV)	β
SW (20:30–20:36)	710	6	2	80	16	1
FS (18:42–18:48)	690	8	2	180	36	2
MS (21:23–21:29)	400	11	5	400	80	7

[Sorriso-Valvo et al., 2010, EPL]

SO(3) decomposition

(Arad et al., 1998; Kurien and Sreenivasan, 2000,2001)

The *n*-th order 3D structure function tensor:

$$S_{\alpha_1,\alpha_2,\ldots,\alpha_n}(l) = \Big\langle \big[B_{\alpha_1}(r+l) - B_{\alpha_1}(r)\big] \times$$

$$\times \big[B_{\alpha_2}(r+l) - B_{\alpha_2}(r)\big] \times \ldots$$

$$\times \big[B_{\alpha_n}(r+l) - B_{\alpha_n}(r)\big] \Big\rangle$$

$\alpha_1=\alpha_2=\ldots\alpha_n=r$ – ordinary n-th structure function

The 2nd order structure function tensor:

$$S_{\alpha\beta},\ (\alpha, \beta = x, y, z)$$

$\alpha \neq \beta$ – purely anisotropic part

$\alpha = \beta$ – both anisotropic and isotropic parts

Scaling properties of anisotropy in the solar wind, foreshock and magnetosheath turbulence

SW

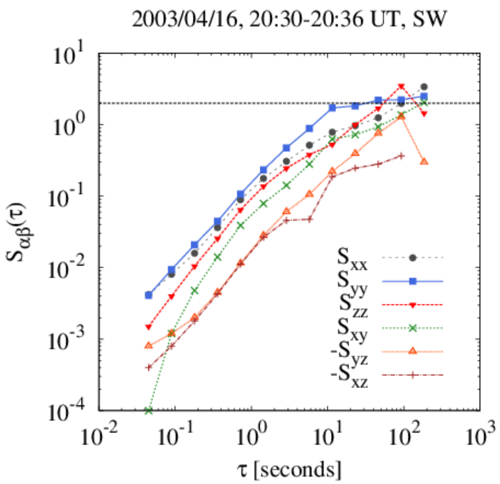

FS

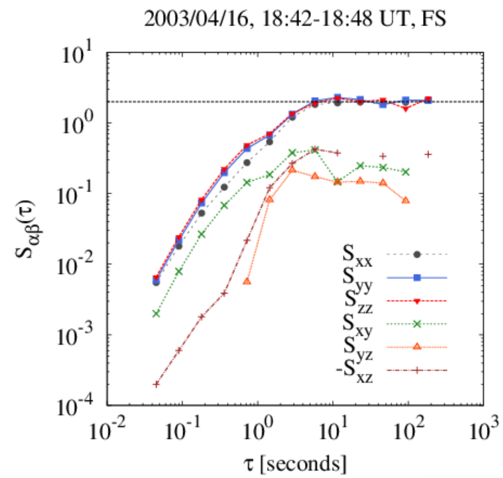

MSH

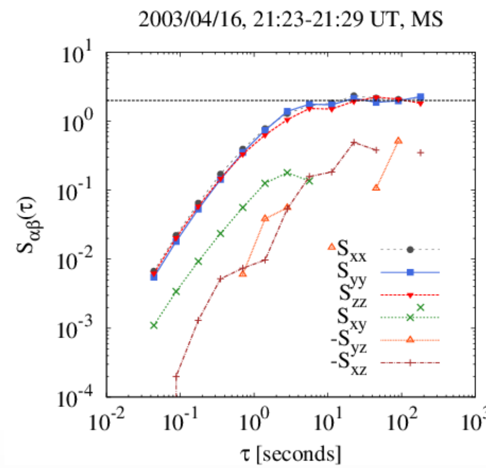

[Sorriso-Valvo, et al., EPL, 2010]

Sxx,yy,zz - isotropic and anisotropic contributions

Sxy,yz,xz - describe the degree of correlations present between the different components of the field fluctuations; *non-vanishing terms* -> anisotropy

Decorellation times - SW - 2 min
FS – 5 sec
MSH – 20 sec

Structure function fit

Batchelor's relation:

$$S_{\alpha_1,\cdots,\alpha_n}(l) = \frac{A_{\alpha_1,\cdots,\alpha_n}\eta^n (l/\eta)^n}{\left[1+B_{\alpha_1,\cdots,\alpha_n}(l/\eta)^2\right]^{C_{\alpha_1,\cdots,\alpha_n}}} \times \left[1+D_{\alpha_1,\cdots,\alpha_n}(l/L_0)\right]^{2C_{\alpha_1,\cdots,\alpha_n}-n}$$

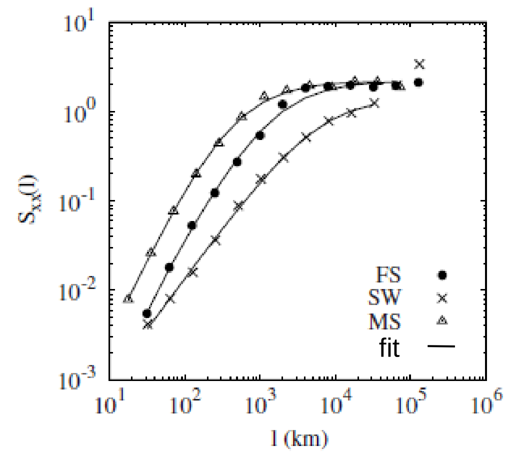

$$L_0 = \frac{\int E(k)k^{-1}dk}{\int E(k)dk}$$

Integral scale

SW ~ 110000
FS ~ 70000
MSH ~ 40000

$$\eta \sim \lambda_T = \sqrt{\frac{\int E(k)dk}{\int E(k)k^2dk}}$$

Dissipation scale

SW – 4000 km
FS – 5000
MSH - 2000

$\zeta_{\alpha_1\alpha_2}$	FS	SW	MS
ζ_{xx}	1.62 ± 0.16	1.15 ± 0.07	1.7 ± 0.1
ζ_{yy}	1.8 ± 0.2	1.0 ± 0.3	1.75 ± 0.18
ζ_{zz}	1.95 ± 0.05	1.7 ± 0.3	1.88 ± 0.06
ζ_{xy}	1.63 ± 0.14	1.37 ± 0.09	1.83 ± 0.06
ζ_{xz}	1.86 ± 0.1	1.0 ± 0.5	1.6 ± 0.3
ζ_{yz}	1.42 ± 0.5	1.0 ± 0.5	1.74 ± 0.2

Relation between ς and C:

$$\zeta_{\alpha_1,\cdots,\alpha_n} = n - 2C_{\alpha_1,\cdots,\alpha_n}$$

Results

The difference between the diagonal and off-diagonal scaling exponents is very small – anisotropy presence at small scales; decay rate comparable to the longitudinal and transverse structure function

Conclusions

- All regions show anisotropic turbulence

- Foreshock and magnetosheath are less anisotropic than the solar wind:

  - due to through the shuffling of the fields occurring in proximity of the bow shock, that could cancel the importance of anisotropy.

  - the presence of a second source of anisotropy (the velocity shear and the other phenomena in proximity of the bow shock) could also contribute to the observed loss of anisotropy.

Two-point structure function of the magnetic field *B*

Single point measurements allow structure function calculation only in the direction of the flow.

Multipoint measurements allow to characterize magnetic field anisotropy at different angles relative to the flow direction.

$$\Delta S_{\alpha\beta}^{12}\left(\vec{l}\right)=\left\langle\left|\vec{B}_{\alpha\beta}^{2}\left(\vec{R}+\vec{l}\right)-\vec{B}_{\alpha\beta}^{1}\left(\vec{l}\right)\right|\right\rangle,\quad \alpha,\beta=x,y,z.$$

$$R\left(\Delta t\right)=d-V_{SW}\Delta t$$

d - initial spacecraft distance
V_{SW} - solar wind speed in plasma frame

2007-01-30, 00:09-00:21 UT, Fast stream

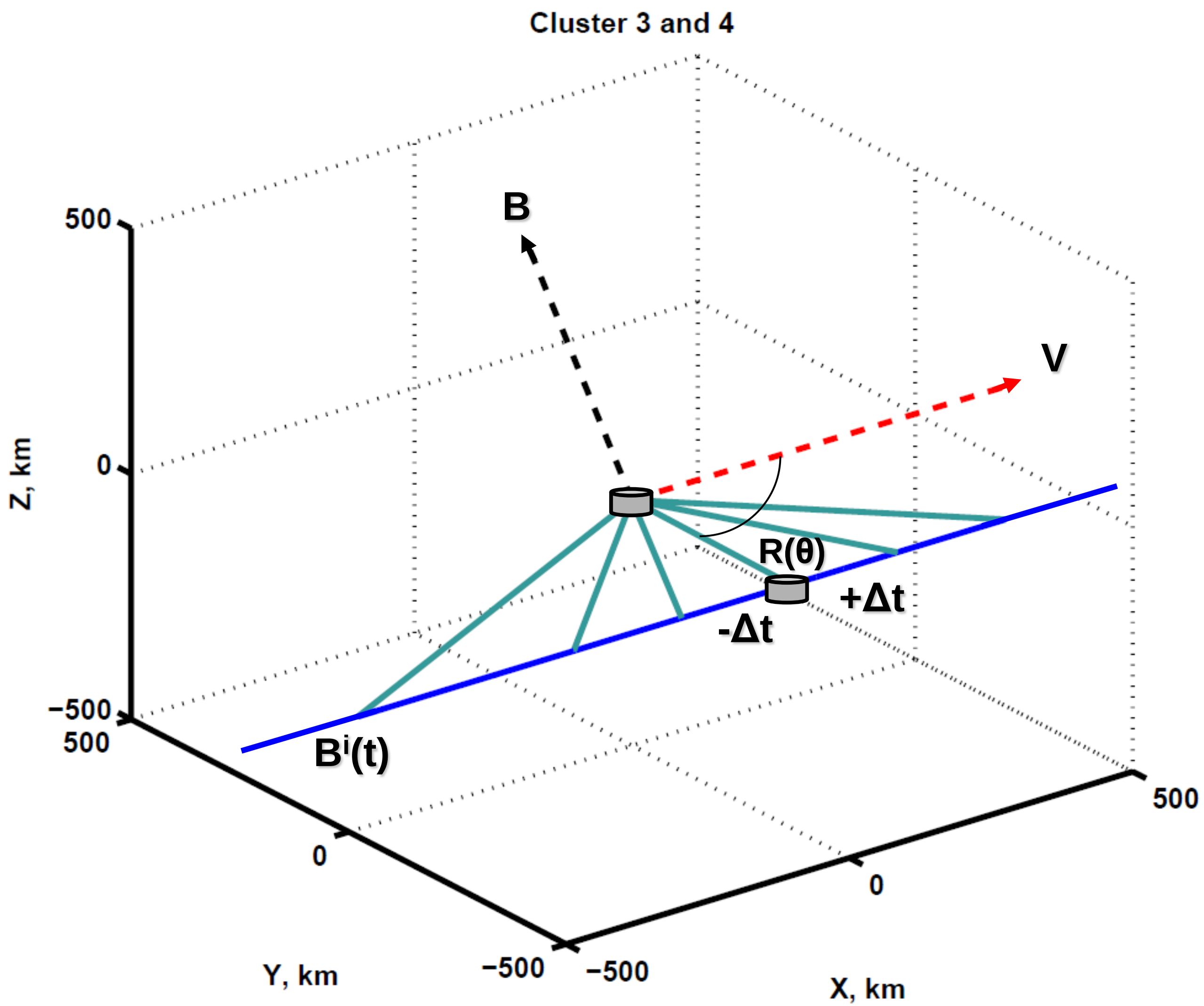

Taylor hypothesis

$$l = -V_{SW}\Delta t$$

$$\frac{\vec{V}_A \Delta t}{\vec{d} - \vec{V}_{SW}\Delta t} \ll 1,$$

$$V_{SW} \gg V_A$$

[Horbury, 2000]

2007-01-30, 00:09-00:21 UT, Fast stream

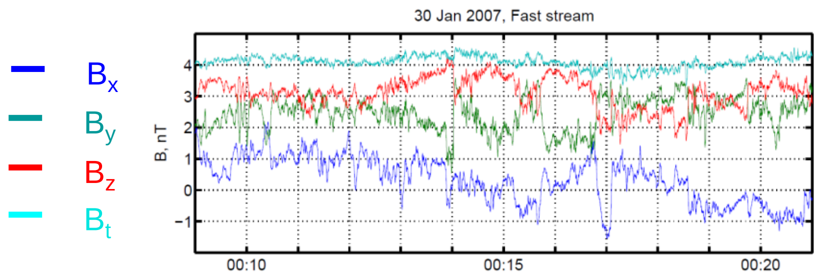

V_{SW}, km/s	*B*, nT	*n*, cm^3
670	4	3

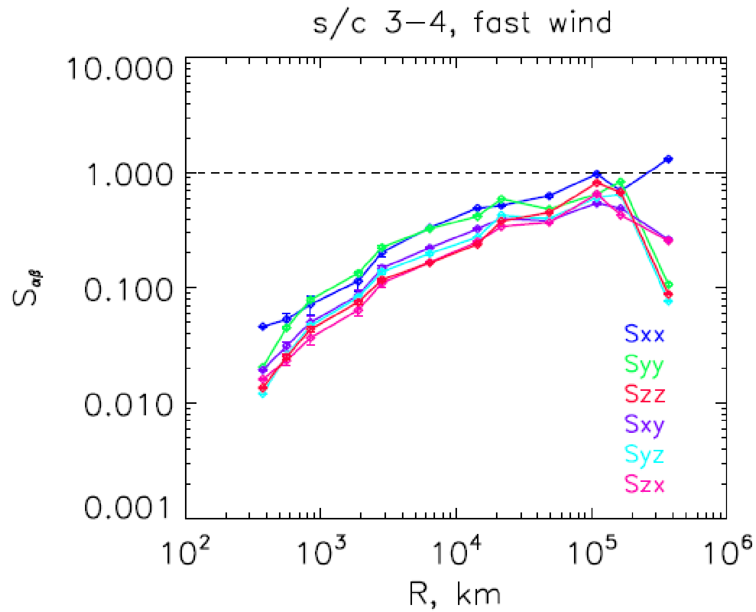

Results

- ❑ non-vanishing anisotropic elements towards the small scales
- ❑ same order in both anisotropic and mixed elements

Conclusions

- ❑ the *return-to-isotropy* assumption does not hold in MHD turbulence
- ❑ the anisotropy is not axisymmetric with respect to the mean magnetic field

Wavelet based partition function (Muzy et al., 1991):

$$Z(q,a) \sim a^{\tau(q)}, \qquad Z(q,a) = \sum_{l \in L(a)} \left(\sup_{a' \le a} \left| T_\psi[g](b_l(a'), a') \right| \right)^q$$

Models

1. P-model (Meneveau & Sreenivasan, '87,'91):

$$\tau(q) = -\log_2 \left[P^{\varsigma_q} - (1-P)^{\varsigma_q} \right]$$

$P_1 = 0.5$ - no intermittency
$P_1=1$ - fully intermittent case

2. Extended SF (Tu et al., '96, Marsh &Tu, '97):

$$\tau(q) = \left(-\frac{5}{2} + \frac{3}{2}\alpha \right) \frac{q}{3} - \log_2 \left[P^{q/3} + (1-P)^{q/3} \right]$$

(Kolmogorov-like cascade)

$$\tau(q) = (-3 + 2\alpha) \frac{q}{4} - \log_2 \left[P^{q/4} + (1-P)^{q/4} \right]$$

(Kraichnan-like cascade)

The Earth's cusp

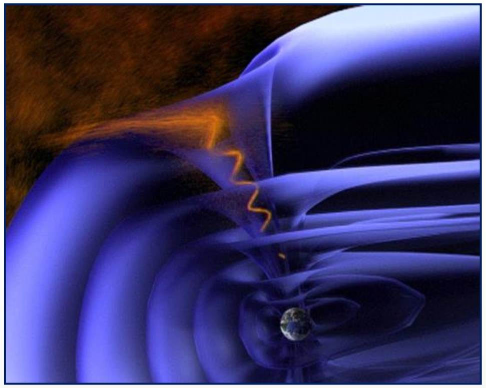

Picture ESA

Results

[Yordanova et al., 2004, Ann. Geoph.]

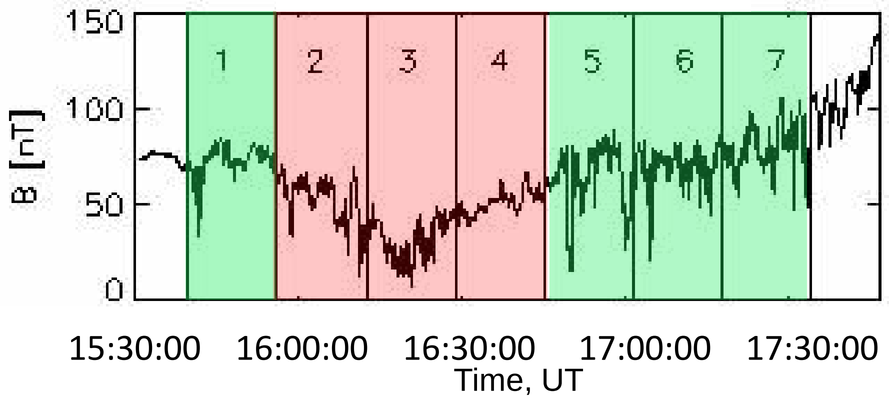

9 Oct 1996

MLat: 55.46 – 70.58
MLT: 12:17 – 12:50
X_{GSM} 3-4 Re, Y_{GSM} 0.5-0.2 Re, Z_{GSM} 7-5 Re

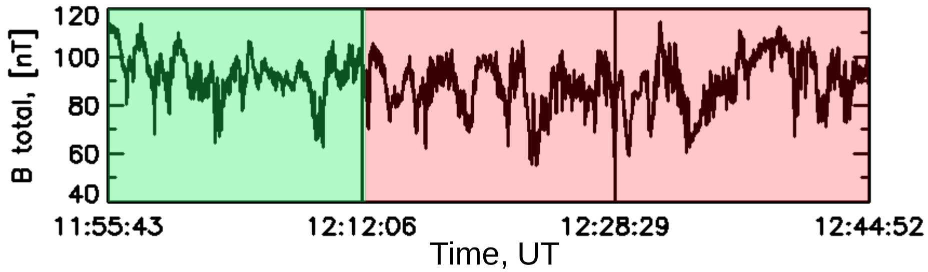

4 Apr 1997

MLat: 59.87° - 67.95 °
MLT: 13:40 - 14:17
X_{GSM} 4.2-3.9 Re, Y_{GSM} 1.5-1.6 Re, Z_{GSM} 5-6 Re

Kolmogorov – like ($B_z < 0$)

Reconnection at subsolar point, plasma flowing on the open field lines towards magnetotail

p – model ($B_z > 0$)

Northern lobe reconnection; turbulent boundary layer - convergence of magnetosheath flow and reconnection associated flow

Power spectra in parallel and perpendicular directions

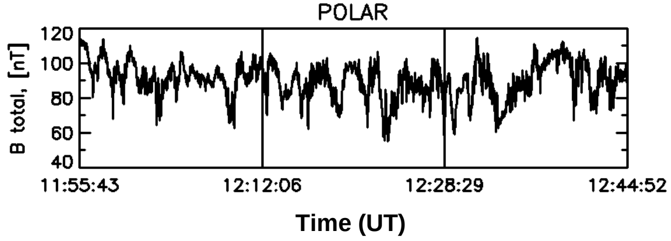

MLat: 61 – 67
MLT: 13:40 – 14:13
d_mp ~ 2-4 Re

B_0 = 91±9 nT
$\delta B_{1,2}$= 0 ± 6 nT

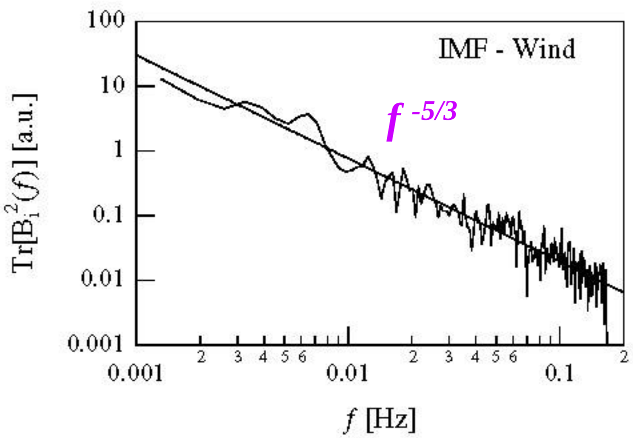

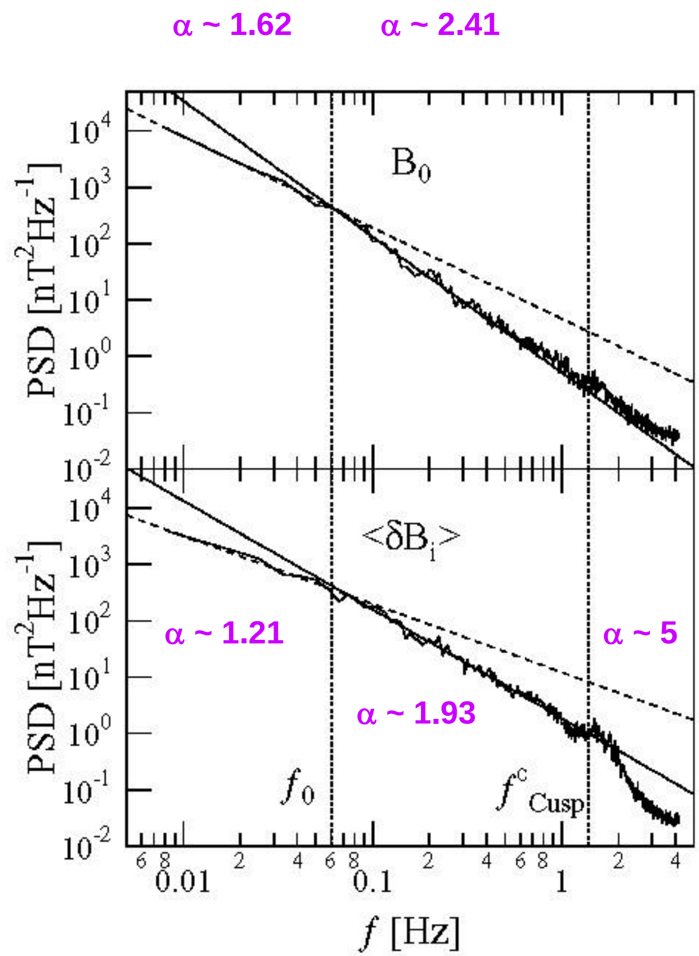

[Yordanova et al., 2005, NPG]

Extended Self-Similarity Analysis

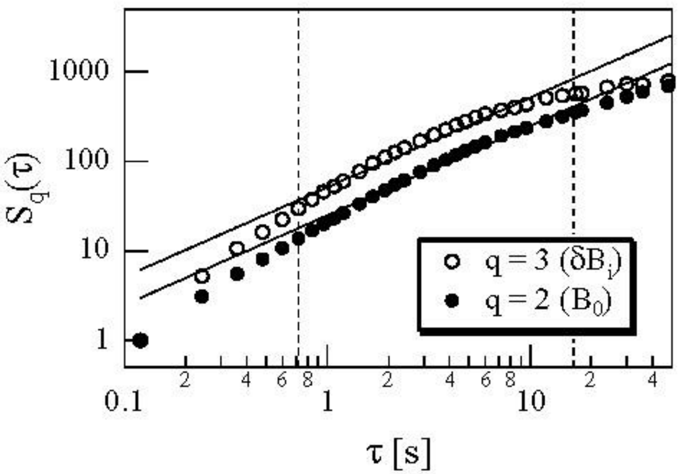

$$S_q(\tau) \sim \left[S_p(\tau)\right]^{\eta_p(q)}$$

$$S_q(\tau) \sim \tau$$

$$\eta_p(q) \equiv \zeta(q)$$

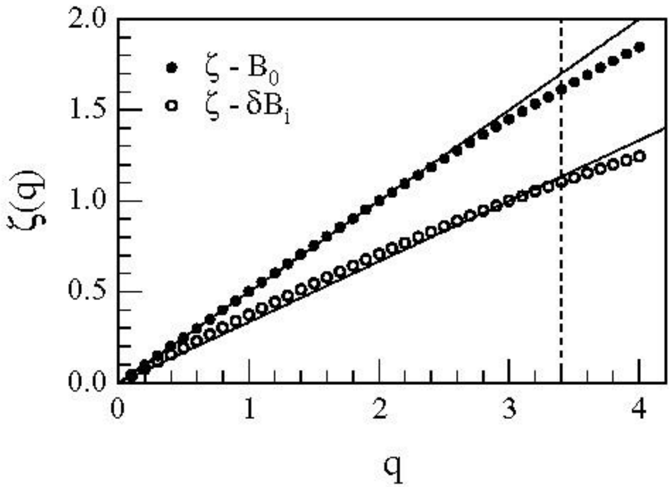

$$S_q(\tau) \sim \left[S_2(\tau)\right]^{\zeta_q} \leftrightarrow B_0$$

$$S_q(\tau) \sim \left[S_3(\tau)\right]^{\zeta_q} \leftrightarrow \delta B_i$$

PDF in parallel and perpendicular directions

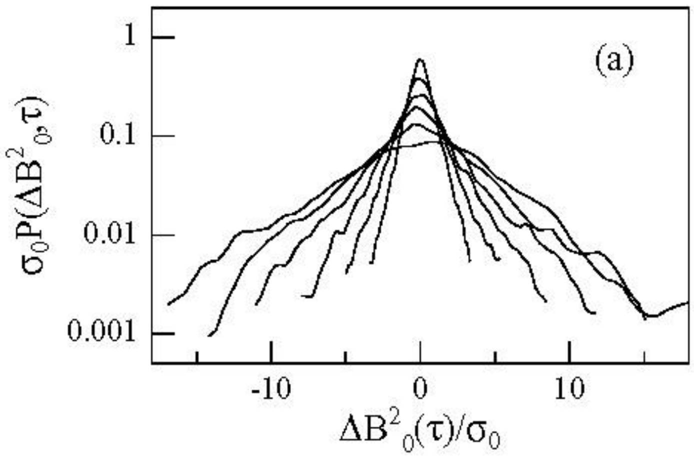

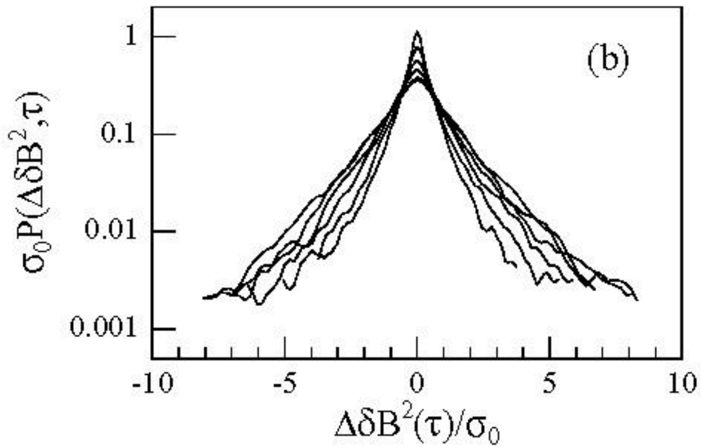

$$\Delta B_0^2 = B_0^2(t+\tau) - B_0^2(t)$$
$$\Delta\delta B^2 = \delta B^2(t+\tau) - \delta B^2(t),$$
$$\delta B^2 = \left(\delta B_1^2 + \delta B_2^2\right)$$

τ= 6, 12, 24, 48, 96, 192Δt

Conclusions

- Magnetic field intensity - turbulence depends on IMF:

  Bz > 0   *p – model*   (*fluid, fully developed*)
  Bz < 0   *Kolmogorov- like*   (*fluid, non-fully developed*)

- Magnetic field components

  PSD - different scaling in parallel and perpendicular directions

  ESS – parallel fluctuations are characterized by quasi-linear (monofractal) nature; perpendicular - by a strong intermittent (multifractal) character

  PDF – more intermittent character of the fluctuations in perpendicular direction then in parallel

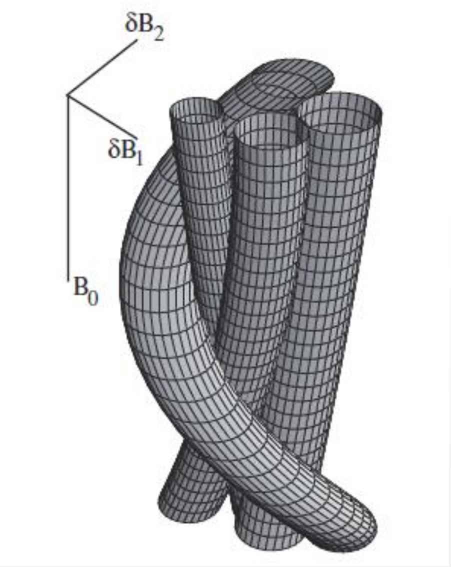

Nonlinear evolution of multi-scale coherent structures

Summary for near Earth's space plasma turbulence

- Solar wind turbulence and the modified turbulence in the near Earth's plasma regions are both intermittent and anisotropic, however to a different degree.

- The nature of turbulence depends on:
  - the source of origin (Solar corona, Bow shock, Magnetopause)
  - local drivers (Stream/stream interactions in the SW; reflected ions in the FS; velocity shears in the MSH and the cusp; reconnection in the cusp)

- Turbulence is more developed away from boundaries

- Anisotropy and intermittency increases away from boundaries